International Journal on Magnetic Particle Imaging
Vol 6, No 2, Suppl 1, Article ID 2009058, 3 Pages

Infinite Science Publishing

Proceedings Article

Blind source separation for multi-color MPI

S. Kurt1[1,2,*] · Y. Muslu1[1,2] · E. U. Saritas1[1,2,3]

[1]Department of Electrical and Electronics Engineering, Bilkent University, Ankara, Turkey
[2]National Magnetic Resonance Research Center (UMRAM), Bilkent University, Ankara, Turkey
[3]Neuroscience Program, Sabuncu Brain Research Center, Bilkent University, Ankara, Turkey
[*]Corresponding author, email: kurt@ee.bilkent.edu.tr

Abstract

In magnetic particle imaging (MPI), different magnetic nanoparticles (MNPs) in the same field-of-view can be distinguished via color-MPI techniques. Existing system-function-based techniques require extensive calibration scans, whereas x-space-based approaches require either multiple scans at different drive field parameters, or rely on the underlying mirror symmetry of the adiabatic MPI signal. In this work, we propose a novel blind source separation technique for multi-color MPI, exploiting the distinct signal delays of different MNPs. The proposed technique blindly decomposes the MPI signals from different MNPs, which can then be individually reconstructed and assigned to separate color channels to form a multi-color MPI image.

I Introduction

Different nanoparticle types can be distinguished via system-function or x-space based multi-color magnetic particle imaging (MPI) techniques. Existing system-function based techniques require extensive calibration scans performed separately for each particle type [1]. X-space based methods require multiple scans at different drive field (DF) parameters [2], or rely on the underlying mirror symmetry of the adiabatic MPI signal [3].

In this work, we propose a blind source separation technique for multi-color MPI, where MPI signals from different sources are blindly decomposed, and the corresponding images are assigned to separate "color channels". The proposed calibration-free technique utilizes a single imaging scan and leverages the differences among the magnetization response delays of different magnetic nanoparticles (MNPs). With imaging results, we show that this technique successfully separates different MNP types.

II Materials and Methods

II.I Theory

As explained in our recent work, a raw MPI image can be formed by sampling the MPI signal at specific positions in the partial field-of-views (pFOVs) and assigning them to pFOV centers [4]:

$$\tilde{\rho}_k(x) = \alpha_k(\hat{\rho}(x) * h_k(x)), \quad k = 1, \ldots, N. \tag{1}$$

Here, $\hat{\rho}(x)$ is the ideal MPI image (i.e., MNP distribution convolved with the point spread function), $\tilde{\rho}_k(x)$ is the raw image formed from the k^{th} positions of the pFOVs, α_k is a constant that depends on the field free point (FFP) speed at the k^{th} position, $h_k(x)$ is a known convolution kernel that depends only on the pFOV size, and N is the number of samples in one cycle.

To estimate the signal delay, we first plot the maximum image intensities of these N raw images, i.e., for each k we compute:

$$\max_x \tilde{\rho}_k(x) = \alpha_k \max_x (\hat{\rho}(x) * h_k(x)) \tag{2}$$

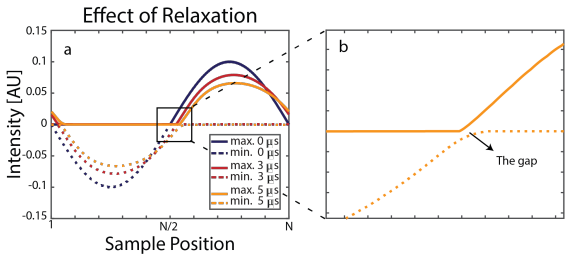

Figure 1: (a) Maximum (solid curves) and minimum (dashed curves) raw image intensities as a function of sample position, k, for three cases: ignoring relaxation, $\tau = 3$ μs, and $\tau = 5$ μs. (b) These two curves do not intersect when τ is non-zero. Simulations were for a point source sample, 2.4 T/m selection field gradient, DF with 10 mT and 9.7 kHz.

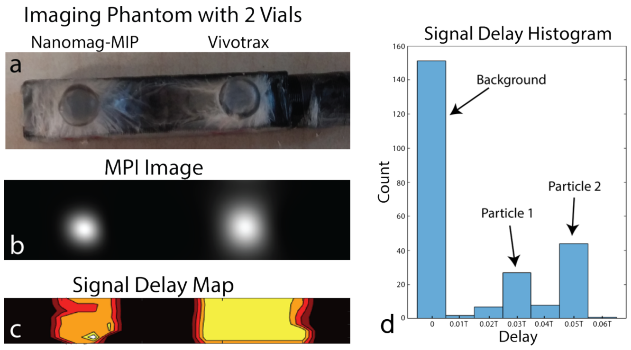

Figure 2: Imaging experiment results. (a) The phantom with 2 vials filled with Nanomag-MIP and Vivotrax. (b) MPI image. (c) Signal delay map and (d) histogram show that there are two distinct MNPs in the FOV. (FOV: 4x0.8 cm^2).

In the absence of signal delays, $\gamma = \max_x(\hat{\rho}(x) * h_k(x))$ is constant for all k, since they are maximum values of the shifted versions of the same image. Therefore, the maximum image intensities without delays depend only on the FFP speed profile, i.e., $\max_x \hat{\rho}(x) = \alpha_k \gamma$. The same is also valid for the minimum image intensities.

Figure 1 shows the maximum and minimum raw image intensities for the case of a point source sample. The MPI signal is simulated first ignoring relaxation, and then for relaxation time constants of $\tau = 3$ μs and $\tau = 5$ μs [5]. The plots dominantly reflect the speed profile of the FFP (i.e., a sinusoidal profile). When relaxation is ignored, the maximum and minimum intensities intersect at $k = N/2$, where both are equal to zero. However, in the case of non-zero τ, the maximum and minimum intensity profiles no longer intersect. We leverage the delay (i.e., the gap) between the maximum and minimum intensity profiles for blind source separation, as different MNPs will have different signal delays.

To get a delay map across the entire FOV, we apply the aforementioned method in local regions, using a moving window approach. For example, if the 2D FOV is covered in 5x11 pFOVs, then a 2x2 moving window can be used to compute local delays, from which a 2D delay map of the FOV can be formed. Next, we create a histogram of the delay map to estimate the number of unique MNP types in the FOV and the corresponding delay values.

Finally, we decompose the MPI signal into signals from different MNPs. As an example, let $s(t) = p_1(t) + p_2(t)$ be the MPI signal that only includes the second harmonic response, and $p_1(t)$ and $p_2(t)$ are the individual signal contributions from two different MNPs, such that

$$p_i(t) = A_I \cos(2\omega(t - t_i)), \quad i = 1, 2. \tag{3}$$

Here, t_i are the signal delays estimated as described above, and A_i are the unknown signal intensities. Let S_2 denote the Fourier transform of $s(t)$ evaluated at the second harmonic. The real and imaginary parts of S_2 provide sufficient information to compute A_i, i.e.,

$$\begin{bmatrix} \cos(2\omega t_1) & \cos(2\omega t_2) \\ \sin(2\omega t_1) & \sin(2\omega t_1) \end{bmatrix} \begin{bmatrix} A_1 \\ A_2 \end{bmatrix} = \begin{bmatrix} 2\,\mathrm{Re}\{S_2\} \\ 2\,\mathrm{Im}\{S_2\} \end{bmatrix}. \tag{4}$$

This 2x2 linear system of equations can be solved to compute A_1 and A_2. Next, by processing $p_1(t)$ and $p_2(t)$ separately, two separate MPI images can be obtained. Finally, these two images can then be assigned to different "color channels" to create a multi-color MPI image. Note that the other harmonics can be processed similarly.

Importantly, the proposed technique is not limited to two MNPs. Each harmonic provides sufficient information to differentiate two additional MNPs (assuming that the MNPs have similar magnetization curves apart from the differences in their signal delays). Hence, using N_h harmonics, one can potentially differentiate up to $2N_h$ different MNPs.

II.II Imaging Experiments

Imaging experiments were performed on our in-house FFP MPI scanner with (-4.8, 2.4, 2.4) T/m selection field gradients in (x, y, z) directions, using a drive field (DF) at 15 mT and 9.7 kHz along the z-direction. The entire FOV was 4x0.8 cm^2, which was covered by a Cartesian trajectory with a 12.5-mm pFOV size, 85 % overlap among pFOVs along the z-direction, and 9 lines along the x-direction. The total scan time was 2 min 14 sec. Nanomag-MIP (Micromod GmbH, Germany) nanoparticles with 1.43 mg Fe/mL and Vivotrax (Magnetic Insight Inc., USA) nanoparticles with 5.5 mg Fe/mL were prepared in 3-mm diameter vials, separated at 15-mm distance (see Fig. 2a). MPI images were reconstructed using an x-space-based reconstruction that we recently proposed, pFOV Center Imaging (PCI) [4].

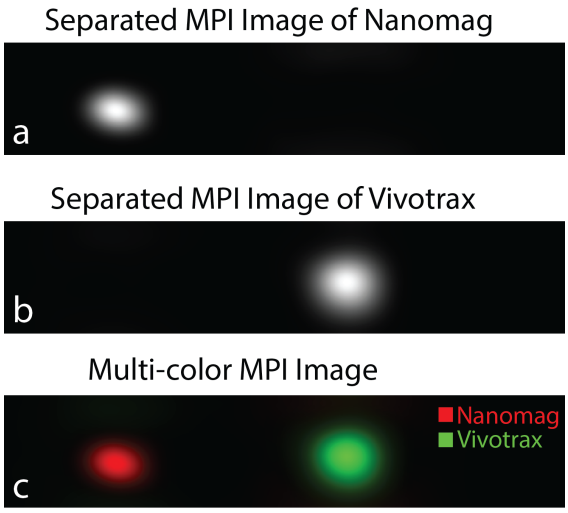

Figure 3: Imaging experiment results for the proposed technique. (a-b) The separated MPI images of Nanomag-MIP and Vivotrax nanoparticles, and (c) multi-color MPI image.

III Results and Discussion

Figure 2 shows the intermediate steps of the proposed blind source separation technique, together with the corresponding MPI image. The signal delay map depicts the local values for the delays, providing a clear distinction between the two MNPs. The delay histogram also indicates the presence of two distinct MNP types.

Figure 3 displays the results of the proposed blind source separation technique, showing successfully separated images of Nanomag-MIP and Vivotrax. For the multi-color MPI image, Nanomag-MIP was assigned to the red channel and Vivotrax was assigned to the green channel.

The proposed technique has important advantages. First, it is a blind, calibration-free technique. In addition, it decomposes the *MPI signal* itself, and not the reconstructed image. Each signal component can then be treated separately to reconstruct individual MPI images of the distinct MNPs. Thus, this technique does not cause any loss of resolution in the separated images. It can also be applied to MNPs under different local environments, as long as the change in environment causes a change in signal delay. Hence, one can reconstruct images of only the regions with specific conditions, e.g., high viscosity or high temperature regions.

IV Conclusions

In this work, a blind source separation technique is presented for decomposing the MPI signals from different MNPs. The decomposed signals can be individually reconstructed and assigned to separate “color channels” to form a multi-color MPI image. This technique can be applied to differentiate MNP types or their local environments.

Author’s Statement

Research funding: This work was supported by the Scientific and Technological Research Council of Turkey (TUBITAK 115E677).

References

[1] J. Rahmer et al., First experimental evidence of the feasibility of multi-color magnetic particle imaging, Phys. Med. Biol., vol. 60, no. 5, pp. 1775–1791, 2015.

[2] D. Hensley et al., Preliminary experimental x-space color MPI, in Proc. 5th Int. Workshop Magn. Part. Imag. (IWMPI), Istanbul, Turkey, Mar. 2015.

[3] Y. Muslu et al., Calibration-free relaxation-based multi-color magnetic particle imaging, IEEE Trans. Med. Imaging, vol. 37, pp. 1920–1931, 2018.

[4] S. Kurt et al., Rapid-PCI: An Alternative X-space Based Image Reconstruction for Rapid Scanning Trajectories, in Proc. 9th Int. Workshop Magn. Part. Imag. (IWMPI), New York, NY, USA, pp. 43-44, Mar. 2019.

[5] L. R. Croft et al., Relaxation in x-space Magnetic Particle Imaging, IEEE Trans. Med. Imaging, vol.31, no.12, pp. 2335-2342, 2012.

